Continuous Cooling Transformation Behavior of High Carbon Pearlitic Steel

Lu-Lu FENG[1,2], Wei-Wen QIAO[2], Jian SUN[3], De-Fa LI[4], Ping-Ping LI[1] and Tian-Dong CAO[1,a,*]

[1]School of Mechanical Engineering, Jing Chu University of Technology, Jingmen 448000, China

[2]Jiangsu Huaneng Cable Co. , Ltd. Gaoyou 225613, China

[3]GuangZhou Guilaxy Mechanical Technology Co.,Ltd. Guangzhou 510000, China

[4]Research Institute of Wuhan Iron & Steel Group, Wuhan 430080, China

[a]838007729@qq.com

*Corresponding author

Abstract. The continuous cooling transformation behavior of high-carbon pearlitic steel was studied by employing optical microscopy, scanning electron microscopy, and the Vickers hardness test. The results show that the microstructure of the test steel is composed of proeutectoid cementite and lamellar pearlite in the cooling rate range of 0.05–2 °C/s and lamellar pearlite in the range of 2–5 °C/s. Further, martensite appears at 10 °C/s. With the increase in the cooling rate, the Vickers hardness of the test steel first decreases and then increases. In the industrial production of high-carbon pearlite steel, the formation of proeutectoid cementite at a low cooling rate needs to be avoided, and at the same time, the formation of martensite and other brittle-phase at a high cooling rate needs to be avoided.

Introduction

High-carbon pearlite steel has excellent comprehensive mechanical properties, and its microstructure is composed of lamellar pearlite or granular pearlite; further, it is often used in constructing bridge cables and precision bearings [1-2]. Due to the high carbon content of high-carbon pearlite steel, proeutectoid cementite often appears in the actual production process, which leads to an increase in the steel hardness and brittleness [3]. The accelerated cooling method is often used to inhibit the emergence of proeutectoid cementite [4]. However, if the cooling rate is too high, brittle structures such as martensite will be produced. In the actual production process, it is necessary to control the cooling rate of high-carbon steel to avoid the appearance of eutectoid cementite and martensite [5]. Currently, there is no relevant report on the effects of continuous cooling of high-carbon pearlite steel. In this study, the continuous cooling transformation behavior of a type of high-carbon pearlitic steel for bridge cables is investigated, and an ideal range of the cooling rate is proposed, which will be beneficial in the practical production of high-carbon pearlite steel.

Experimental Methods

Experimental materials to produce a Φ 14-mm wire rod mill and the chemical composition of the test steel specimen are as shown in Table 1. With the method of machining processing Φ 6 x 70 mm style, in Gleebel - 2000 thermal simulator simulation test the continuous cooling transformation (CCT) behavior of steel, with 10 °C/s heating speed from room temperature heating up to 1200 °C isothermal 5 min austenitizing, then with 10 °C/s cold quickly cooled to 950 °C, heat preservation after 10 s to 0.5 °C/s, 0.1 °C/s, 0.2 °C/s, 0.5 °C/s, 1 °C/s, 2 °C/s and the cooling speed of 5 °C/s cool to room temperature. By optical microscope (OM, Olympus BM51) and scanning electron microscope (SEM, Sirion 200) microstructure morphology observation test of steel, volume

expansion method is used to determine the phase transformation point and combining the test steel under different cooling rate on microstructure morphology to determine phase transformation temperature, according to the phase transformation point map test steel CCT curves, with low load Vickers hardness tester (NV1–10A) measure Vickers hardness HV10 test steel.

Results

Continuous Cooling Transition Curve of Test Steel. The CCT curve of the steel is shown in Fig. 1. The cooling curve number represents the cooling speed, from the cooling curve, the cooling speed in 0.05 2 °C/s first eutectoid cementite occur from time to tome, cooling speed greater than 2 °C/s first eutectoid cementite disappeared, after test steel into cementite of ferrite and pearlite, equally between 2–10 °C/s into pearlite organization.
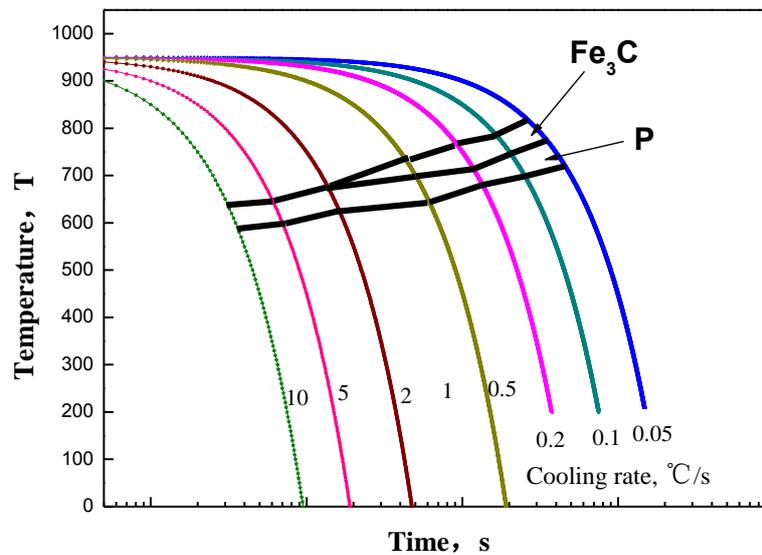

Fig.1 Continuous cooling transformation curve of test steels

Microstructure of the Tested Steel. The microstructure of the test steel is shown in Fig. 2 and Fig. 3. Fig. 2 (a) and Fig. 3 (a) show that pre-eutectoid cementite is obtained during cooling at 0.05 °C/s, which is indicated by the red arrow. This is because, at the low cooling rate, pre-eutectoid transformation occurs in the high-temperature zone above the eutectoid transformation temperature of high-carbon steel, and thus, proeutectoid cementite is formed [6]. In the subsequent cooling process, the untransformed undercooled austenite undergoes eutectoid transformation to form lamellar pearlite [7]. Similarly, when the cooling rate is 0.1–2 °C/s, the transformation of undercooled austenite of the test steel is the same as that at the cooling rate of 0.05 °C/s. The transformation structure is proeutectoid cementite and lamellar pearlite, as shown in Fig. 2 (b)–(d) and Fig. 3 (b)–(d). When the cooling rate is greater than 2 °C/s, the proeutectoid transformation of undercooled austenite is inhibited, the proeutectoid cementite disappears [8], and the test steel structure transforms into the complete lamellar pearlite structure, as shown in Fig. 2 (e) and (f) and Fig. 3 (e) and (f). The lamellar pearlite spacing also changes with the increase in the cooling rate. Fig. 3 (e) and (f) show that the lamellar spacing of pearlite decreases obviously with the increase in the cooling rate.
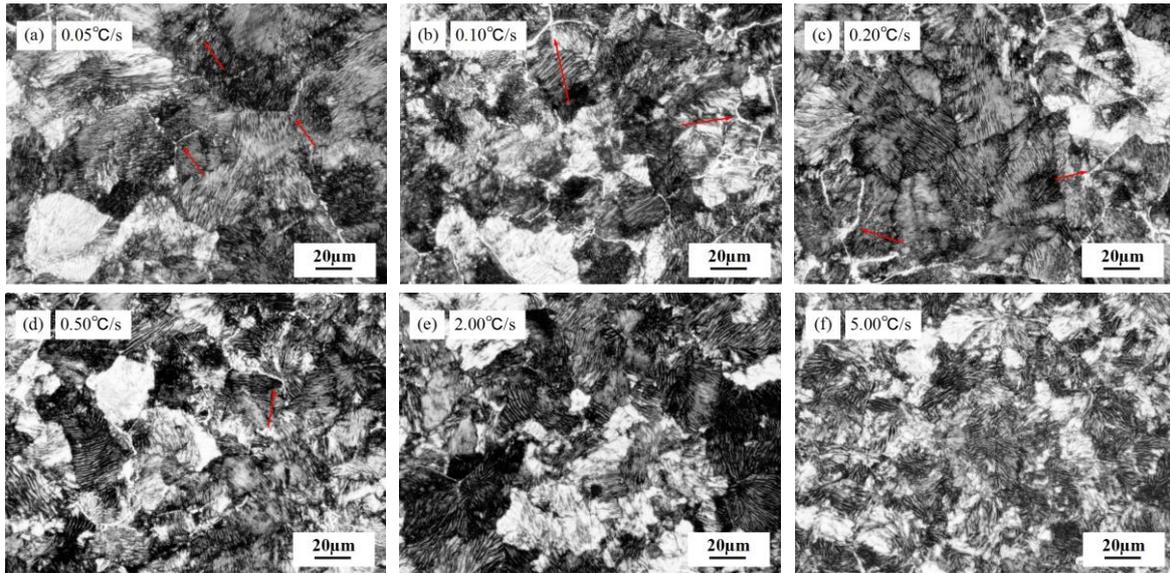
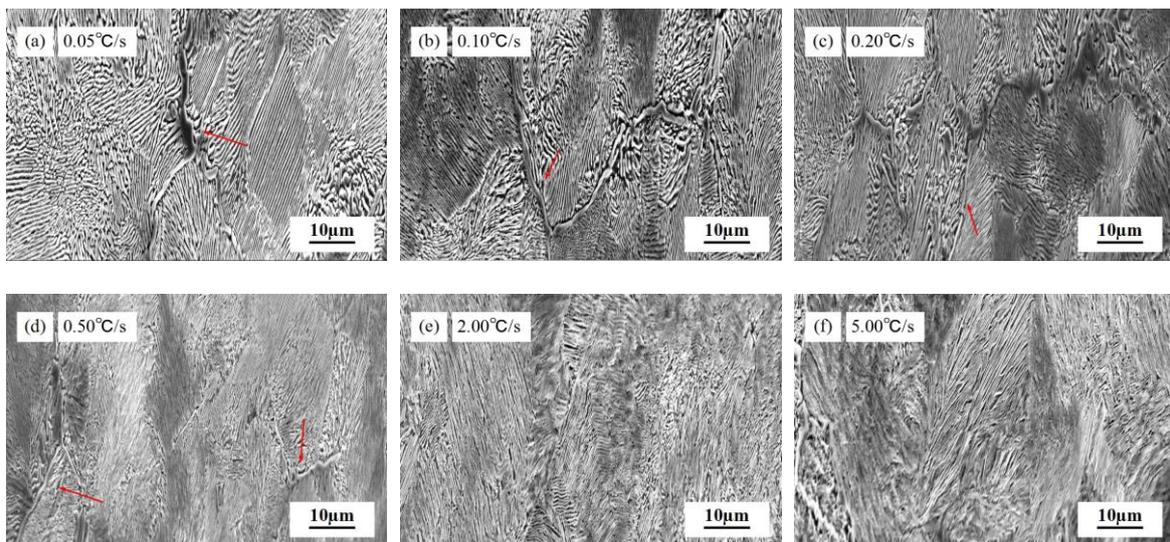Fig.2 Microstructure of test steel at different cooling rates

Fig.3 SEM photo of test steel at different cooling rates

Microstructure Transformation of Test Steel Under Rapid Cooling. The microstructure morphology of the test steel at the cooling rate of 10 °C/s is shown in Fig. 4. The lamellar pearlite structure of the test steel is obtained at the cooling rate of 5 °C/s, but when the cooling rate reaches 10 °C/s. The reason for this is that with the increase in the cooling rate, the temperature decreases too rapidly, and some carbon in the undercooled austenite does not have sufficient time to diffuse; therefore, the diffusion-type transformation cannot occur [9]. As shown in Fig. 4 (b), the morphology of austenite is obviously different from that of lamellar pearlite.
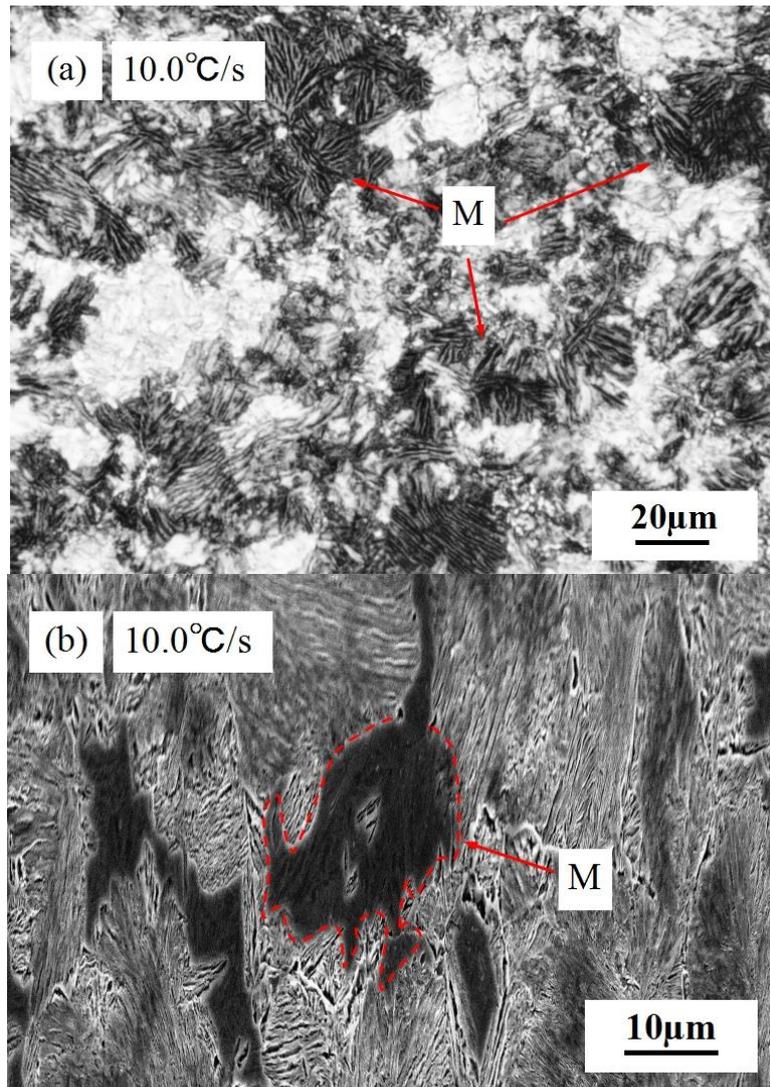
Fig.4 Microstructure of test steel at 10 ℃ / s

Relationship between Cooling Rate and Hardness. Fig. 5 shows the relationship between Vickers hardness and the cooling rate of the test steel. It can be seen from the figure that the Vickers hardness decreases with decreasing cooling rate, which is due to the appearance of proeutectoid cementite in the test steel and high hardness at a low cooling rate [10]. With the increase in the cooling rate, the proeutectoid cementite disappears, and the hardness decreases, but when the cooling rate reaches 10 ℃/s, the Vickers hardness increases, which is due to the appearance of martensite in the microstructure with the increase in the cooling rate, which increases the hardness of the test steel.
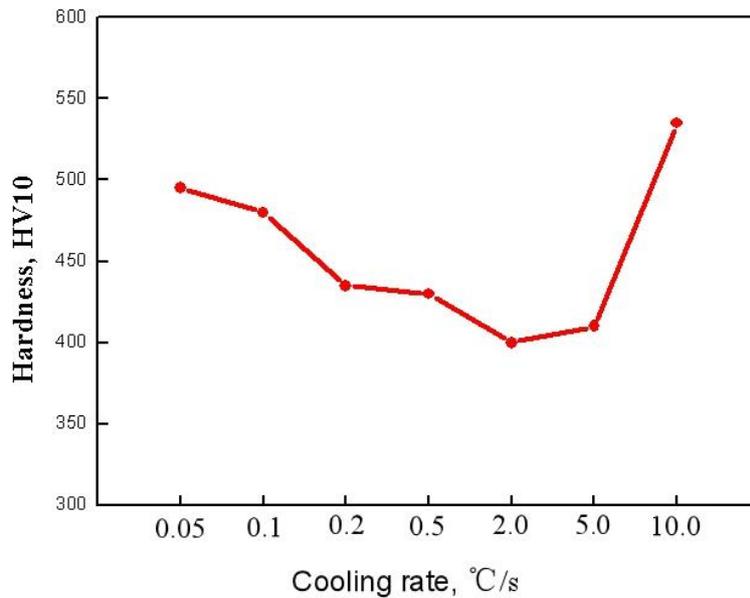
Fig.5 Relationship between Vickers hardness and cooling rate of test steel

Conclusion

1) The microstructure of the test steel shows proeutectoid cementite and lamellar pearlite in the cooling rate range of 0.05–2 °C/s and lamellar pearlite in the range of 2–5 °C/s. Further, martensite appears at 10 °C/s.

   2) In industrial production, the cooling rate of high-carbon-steel wire rod should be accelerated to prevent the formation of eutectoid cementite. Further, to avoid the appearance of a brittle structure with high hardness, such as martensite, which deteriorates the service performance of the product, the cooling rate should not be too high. The ideal cooling rate range is 2–5 °C/s.

Acknowledgement

References

[1] Christine B and Reiner K 2016 *Prog Mater Sci* 82 405

[2] Bhadeshia H K D H 2012 *Prog Mater Sci* 57(2) 268

[3] Han H B, Zhao X M and Zhao X Y 2017 *Metall res Technol* 14(2) 208

[4] Wang Y L, Yu W and Chen Y L 2020 *Mater Res Express* 7(11) 116508

[5] Li Z X, Li C S and Ren J Y 2018 *Metall Mater Trans A* 49(5) 1782

[6] Shamsher S, B Narender M S and Rajendra M B 2016 *Mater Today Procee* 3(6) 1553

[7] Caballero F G, Capdevila C and García C 2000 *Scripta Mater* 42(6) 537

[8] Li Y J, Choi E and Borchers 2011 *Acta Mater* 50 3965

[9] Li Y J, Choi P and Goto S 2012 *Acta Mater* 60 4005

[10]Khalid F A, Edmonds D V1997 *J Mater Process Tech* 72 434